Thermal, optical, interfacial and mechanical properties of titanium dioxide/shape memory polyurethane nanocomposites

Shuang Shi, Dongya Shen, Tao Xu, Yuqing Zhang

PII: S0266-3538(18)30357-9

DOI: 10.1016/j.compscitech.2018.05.022

Reference: CSTE 7225

To appear in: *Composites Science and Technology*

Received Date: 11 February 2018

Revised Date: 2 May 2018

Accepted Date: 12 May 2018

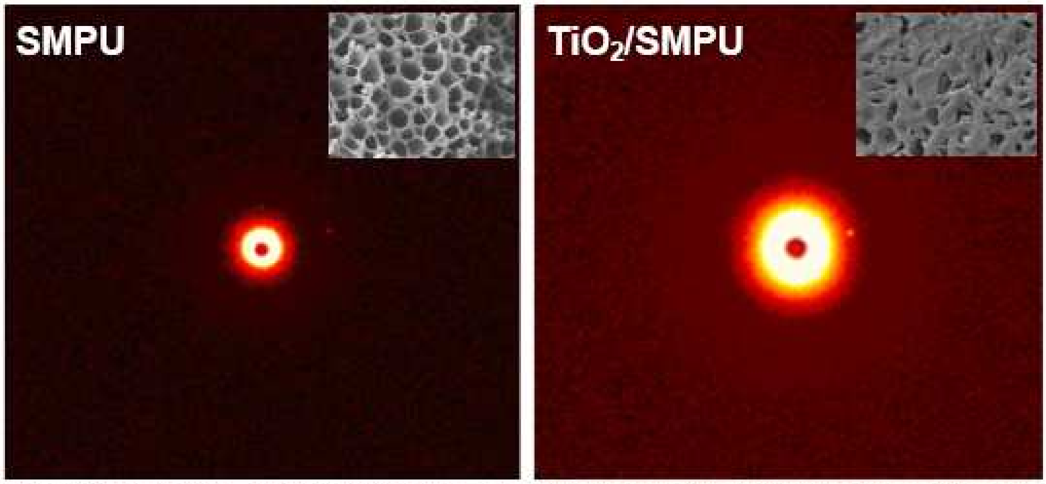

2D-SAXS patterns and SEM images of SMPU and TiO_2/SMPU nanocomposites

Thermal, optical, interfacial and mechanical properties of titanium dioxide/shape memory polyurethane nanocomposites

Shuang Shi[1], Dongya Shen[1], Tao Xu[1]*, Yuqing Zhang[2]

[1] School of Civil Engineering, Nanjing Forestry University, 159, Longpan Road, Nanjing 210037, Jiangsu, China

[2] School of Engineering and Applied Science, Aston University, MB153A, Aston Triangle, Birmingham, B4 7ET, U.K.

*****Corresponding author E-mail: seuxt@hotmail.com

Abstract: To further understand effects of titanium dioxide (TiO_2) nanoparticles on thermal, optical, microstructural, interfacial and mechanical properties of shape memory polyurethane (SMPU), TiO_2/SMPU nanocomposites with different TiO_2 contents were synthesized. Then various properties of TiO_2/SMPU nanocomposites were characterized. Results indicate that the melting temperature of soft segments in SMPU can be used as the shape memory transition temperature of TiO_2/SMPU nanocomposites. TiO_2 nanoparticles are almost filled in SMPU pores to form compact skeleton structures in TiO_2/SMPU when the TiO_2 content is 3% by weight. Further, the used TiO_2 is rutile phase, and lowers the SMPU crystallinity. The suitable TiO_2 content can increase the absorptivity to UV light and enhance the reflectivity to visible light of TiO_2/SMPU nanocomposites, lowering its photo-aging properties and prolonging its service life. Also, TiO_2/SMPU shows a higher scattering intensity and a faster decreasing trend than SMPU due to the larger electron density difference between TiO_2 and SMPU. The microphase separation and ordered structures in SMPU are decreased due to added TiO_2 nanoparticles. There are electron density fluctuations at the interfaces between hard and soft phases in SMPU, and between SMPU and TiO_2 nanoparticles. Finally, the prpared TiO_2/SMPU nanocomposites have better shape memory effects and tensile properties when TiO_2 content of 3% is proposed to synthesize TiO_2/SMPU nanocomposites for practical engineering applications.

Keywords: A. Particle-reinforced composites; B. Environmental degradation; B. Interface; B. Mechanical properties; B. Thermal properties

1. Introduction

TiO_2 is widely used in environmental applications, cosmetics, paper, coatings, foods, toothpastes and paint because of its green, clean, low cost and sustainable innovation [1]. During the past several decades, TiO_2 has been extensively studied due to its interesting electric, magnetic, catalytic, and electrochemical properties [2]. TiO_2 has three distinct polymorphs, including rutile, anatase and brookite. Anatase TiO_2 is adapted to photocatalytic applications, and rutile TiO_2 exhibits a high refractive index and hiding power, as well as good chemical stability and UV light screening effects [3].

Additionally, TiO_2 is a wide band-gap semiconductor with a high refractive index, which lends it to be used as a whitening agent. TiO_2 is also an effective opacifier when used as powder [4]. The scattering power of individual TiO_2 particles for visible light is maximized when the particles have a diameter of approximately 300 nm [4]. Man et al. [5] investigated effects of TiO_2 on optical and mechanical properties of poly (lactic acid) to understand the UV shielding role of TiO_2 additives on the stability of polymer based nanocomposites. Finally, TiO_2 is often used as the reinforcement phase of polymer matrix to improve its mechanical properties.

Recently, as a smart material, shape-memory polymers (SMPs) can change their shape in response to external stimuli such as heat, light, electric or magnetic field [6]. SMPs have many advantages over shape memory alloys in easy processing, low density, high shape recovery, high recoverable strain, and low manufacturing cost [7]. In particular, the thermally actuated SMPs have received more and more attention in recent years due to their potential applications. SMPs usually include the cross-links to determine the permanent shape, and the switching segments with transition temperature (T_t) to fix the temporary shape [8]. According to the nature of switching segments, SMPs are further subdivided into two categories, including SMPs with amorphous switching segments where T_t is the glass transition temperature (T_g), and

SMPs with crystalline switching segments, where T_t is the melting temperature (T_m) [8].

Among these SMPs, SMPUs have attracted more and more attention during the past decades because of their excellent properties such as high tensile strength, high flexibility, high abrasion resistance, good adhesion ability, and so on [9]. SMPUs have become one of the most rapidly developing members of PU industry, and have been applied in many aspects such as coatings, textiles, adhesives, sealant, films, etc [10]. However, SMPU still has such limitations as lower stiffness and weaker shape recovery force when compared with shape memory alloys and ceramics [9]. Further, like other polymer materials, SMPU is vulnerable to aging and ultimately fails to meet the performance requirements and subsequently limits its practical application when exposed to heat, oxygen or ultraviolet (UV) light during its service life. All these result from the age hardening and sacrifice of desirable physical properties of SMPU.

Considerable efforts were made to exploit the potential of nanocomposites and nanoscale materials in both academic and industrial community. One of important approaches consists in the reinforcement of SMPU using fibers and inorganic nanoparticles, such as TiO_2, Al_2O_3, silica, clay, etc [11]. Among these nanoparticles, TiO_2 have recently received an increasing attention due to its many valuable properties cited above. Zhou et al. [12] reported a novel thermal-sensitive polyurethane/TiO_2 nanohybrid membrane prepared via in situ process, and discussed its thermal sensitive characteristics. Chen et al. [13] prepared the thermo-sensitive polyurethane solution containing different TiO_2 concentrations, and found that gas permeability coefficients of membranes to increase with the increase in TiO_2 concentration.

More recently, Zhang et al. [14] studied the influence of anisotropic TiO_2 nanoparticles on the structure formation in a semicrystalline isotactic polypropylene. TiO_2 nanoparticles increased the elastic modulus of isotactic polypropylene and improve environmental stability by attenuating UV light that degrades the polymer. Marzouk et al. [15] discussed the effect of TiO_2 on the optical, structural and crystallization behavior of barium borate glasses. Ramos et al. [16] studied the mechanical and physicochemical characteristics of chitin hydrogels reinforced with TiO_2 nanoparticles, and found TiO_2 endowed chitin gels mechanical stability.

It is noted that some properties of pure SMPU do not quite meet the requirements of engineering materials. However, few studies involved in influences of TiO_2 nanoparticles on the thermal, optical, microstructural, interfacial, shape memory and mechanical properties of SMPU. Further, the interactions and interfacial structures between TiO_2 nanoparticles and SMPU matrix were seldom reported. How to utilize the merits of TiO_2 to comprehensively improve various properties of SMPU is seldom investigated. The objective of this study is to understand effects of TiO_2 nanoparticles on thermal stability, crystallization behaviors, photo-aging property, microstructure, interfacial structure, shape memory effects and mechanical performance of SMPU, and then a suitable TiO_2 content is proposed to prepare TiO_2/SMPU nanocomposites, meeting the requirements of practical engineering materials.

In this study, TiO_2/SMPU nanocomposites with different TiO_2 contents were first synthesized by in-situ polymerization method. A differential scanning calorimeter (DSC) was used to discuss effects of different TiO_2 contents on the thermal properties of SMPU, and to determine the T_t for programming the nanocomposites. Then field emission scanning electron microscopy (FESEM) were utilized to observe the microscopic morphology changes of TiO_2/SMPU, respectively. Also, optical properties of TiO_2/SMPU nanocomposites were characterized using ultraviolet-visible light diffuse reflectance spectra (UV-vis DRS) to discuss effects of TiO_2 contents on the photo-aging property of SMPU. After that, crystallization behavior changes of SMPU and interfacial structures between TiO_2 and SMPU were characterized using wide angle X-ray diffraction (WAXD) and small angle X-ray scattering (SAXS) after the addition of TiO_2, respectively. Finally, influences of TiO_2 contents on shape memory effects and mechanical properties of

SMPU were investigated to validate whether the prepared TiO_2/SMPU can meet the requirements of practical engineering application. Then the suitable content of TiO_2 was proposed to synthesize TiO_2/SMPU nanocomposites for practical engineering applications.

2. Experimental

2.1 Synthesis of samples

The nanocomposites were synthesized by dispersing TiO_2 nanoparticles in SMPU matrix using the in-situ polymerization. Firstly, the calculated amount of Poly-1, 4-butylene adipate glycol (PBAG, Suzhou Xuchuan Chemical Co. Ltd., China, M_n=2000) was put into the flask which was equipped with a thermometer, a mechanical stirrer, nitrogen inlet and outlet tubes. The temperature was slowly elevated to 120 ^oC, and this temperature was maintained for 1.5 h for vacuum dehydration where the vacuum degree was more than 0.095 MPa.

Secondly, the calculated amount of 2, 4-tolylene diisocyanate (TDI, Shanghai TCI Chemical Co. Ltd., China) was added when the temperature was slowly dropped to 80 ^oC. The reaction took place for 2 h under the protection of nitrogen. Thus the SMPU pre-polymer was obtained. Thirdly, TiO_2 nanoparticles with the particle size of 30 nm (Xuancheng Jingrui New Material, Co. Ltd., China,) was added and blended quickly with the mechanical stirring for about 10 minutes at 80 ^oC to be dispersed uniformly in the pre-polymer. Fourthly, when the temperature was further slowly dropped to 70 ^oC, the calculated amount of 1, 4-Butanediol (BDO, Sinopharm Chemical Reagent Co. Ltd., China) was added dropwise into the mixture with the quick stirring for 30 min for chain extension.

Finally, after the reaction was completed, the nanocomposites were injected into a polytetrafluoroethylene mold where the homogeneous mixture was cooled to room temperature and cured. Thus the TiO_2/SMPU samples were obtained after demoulding. Then these nanocomposite samples were subjected to different experiments for characterizing their various properties. The prepared samples were marked as SMPU, 1% TiO_2/SMPU, 3%TiO_2/SMPU, 5%TiO_2/SMPU, which represented the ratios of TiO_2 to SMPU pre-polymer were 0%, 1%, 3%, 5% by weight, respectively.

2.2 Characterization method

A DSC (204F1 type, Netzsch, Germany) was used to analyze effects of TiO_2 contents on T_t of the SMPU under nitrogen atmosphere. Approximately 10 mg sample was heated from −20 ^oC to 100 ^oC at a heating rate of 10 ^oC/min. Subsequently, the temperature was dropped to −20 ^oC with a cooling rate of 20 ^oC/min. Once again, the sample was heated to 100 °C at a heating rate of 10 ^oC/min.

FESEM (JSM-7600F type, JEOL, Japan) was used to observe microscopic morphology characteristics of SMPU and TiO_2/SMPU nanocomposites, respectively. Samples were first fixed on an aluminum sample stub and sputtered with gold under vacuum conditions. Then the sample chamber was opened to place samples. Finally, the morphologies of samples were observed using FESEM.

A UV-vis spectrophotometer (Lambda 950 type, PE, USA) was utilized to record the diffuse reflectance spectra of SMPU and TiO_2/SMPU samples. A $BaSO_4$ standard was used as a reference sample for baseline correction. The scan range was 200–800 nm at a data interval of 1nm.

WAXD (Ultima IV type, Rigaku, Japan) was used to investigate effects of TiO_2 contents on the crystallization behaviors of SMPU. The XRD analyzer was with Cu-Kα radiation (λ= 0.15418 nm). The accelerating voltage and applied current were 40 kV and 30 mA, respectively. The WAXD patterns were recorded in the 2θ range from 10 ° to 80 ° in the step scanning mode at a rate of 2°/min.

The effects of TiO_2 addition on molecular chain states of hard and soft segments in SMPU and interfacial structures between TiO_2 nanoparticles and SMPU matrix were characterized using a SAXS instrument (Nanostar type, Bruker AXS, Germany) with Cu-Kα radiation and Ni chip filtering, respectively. The accelerating voltage and applied current were 35 kV and 30 mA, respectively. The step scanning mode was used with a step length of 0. 02° at a scanning rate of 1° min^{-1}.

The influence of TiO_2 contents on the shape memory effects of SMPU was evaluated at (Tt+10) °C using the shape fixity ratio (R_f) and shape recovery ratio (R_r) which were described elsewhere [17].

Dog bone specimens with the middle distance of 40 mm were stretched by an electronic universal testing machine (ETM504C, Wance test equipment, China) to study the influence of TiO_2 content on the tensile properties of the SMPU. The tensile properties, such as tensile strength and elongation at break, were tested at room temperature with a loading rate of 10 mm/min. Three effective specimens were tested for each group.

3. Results and discussion

3.1 Thermal properties

DSC tests were conducted to discuss effects of different TiO_2 contents on the thermal properties of TiO_2/SMPU nanocomposites. The test results are shown in Fig. 1.

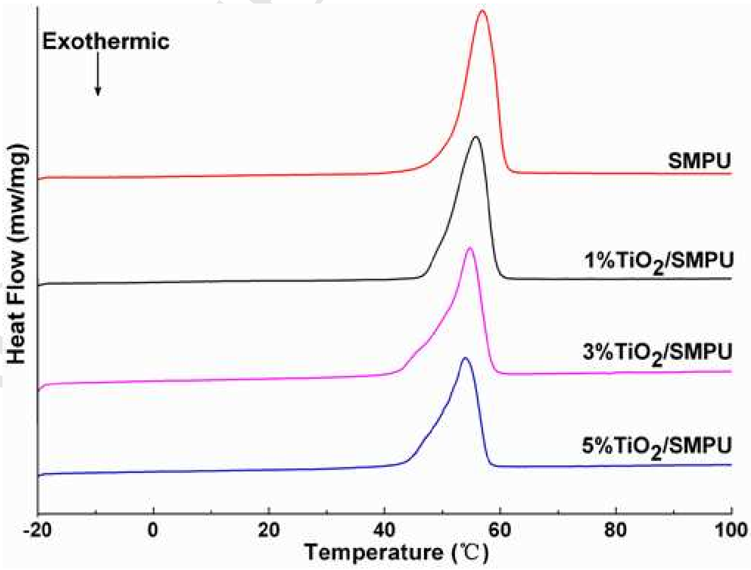

Fig. 1 DSC thermograms of TiO_2/SMPU nanocomposites with different TiO_2 contents

From Fig. 1, the obvious step-shape changing curves are not seen on DSC thermograms, so it is difficult to determine the T_g of TiO_2/SMPU nanocomposites. However, TiO_2/SMPU samples show endothermic peaks in the temperature range from 40 ^{o}C to 65 ^{o}C, which suggests the T_m of crystallites in soft phase of SMPU. This is because the T_m of hard phase in SMPU is usually higher than this temperature range [18]. It is believed that the endothermic peaks are the melting peaks of soft phase or the overlaps of hysteretic peaks of T_g [19]. Since the shape memory is generated by the entropy elastic behavior of rubbery soft phase, T_m of soft phase is generally regarded as T_t of SMPU to actuate its shape memory actions [20]. Therefore, DSC thermograms determine the T_ts of crystalline soft segments as the shape memory switching temperature of TiO_2/SMPU to discuss their shape memory properties [20].

Additionally, it is noted that the DSC curve peak shows a slight shift to the low temperature with the increase in TiO_2 contents, indicating that the T_ts of TiO_2/SMPU nanocomposites are gradually lowered. This is attributed to the fact that the added TiO_2 nanoparticles disturb the symmetry and orderness of SMPU molecular chains, and hinders the crystallization of soft phases which causes the decrease in crystallinity of SMPU [21]. Thus the T_ts of TiO_2/SMPU are lowered as the TiO_2 content is increased. However, it is found that TiO_2 content shows slight influences on the T_t of TiO_2/SMPU nanocomposites.

3.2 Morphology changes

FESEM was used to discuss the changes in microscopic morphology of TiO_2/SMPU nanocomposites as the TiO_2 content is increased. SEM images of TiO_2/SMPU nanocomposites with different TiO_2 contents are present in Fig. 2.

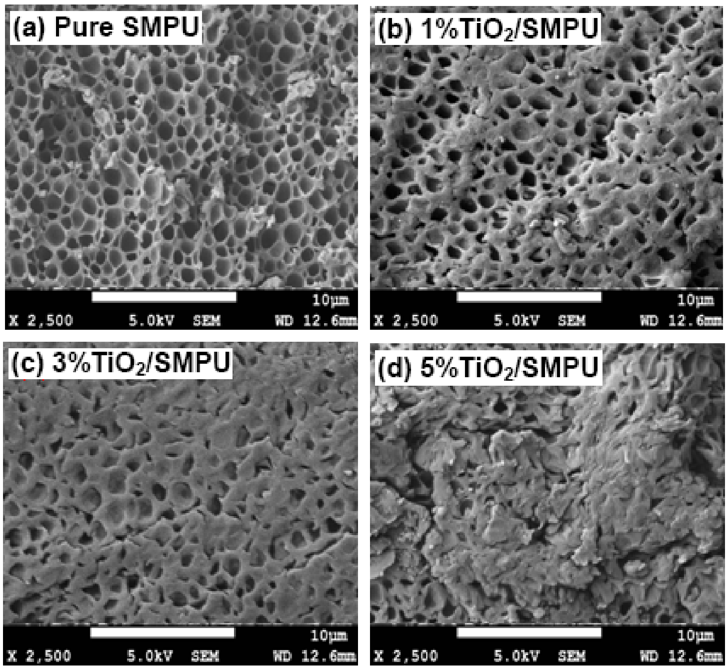

Fig. 2 SEM images of TiO_2/SMPU nanocomposites with different TiO_2 contents

It is seen from Fig.2 (a) that pure SMPU is composed of a lot of porous structures. The applied loads can be delivered by the pore walls in TiO_2/SMPU nanocomposites. However, the pores in SMPU are gradually filled up by TiO_2 nanoparticles with the increase in TiO_2 content. As shown in Fig. 2 (b), the pores are partly filled up when the TiO_2 content is 1%. From Fig. 2 (c), it is observed that all pores are almost filled up and few agglomerations are found when TiO_2 content is 3%. TiO_2 nanoparticles are wrapped by SMPU matrix to form a compact skeleton structure in TiO_2/SMPU nanocomposites. However, when TiO_2 content is up to 5%, the microscopic morphology is not smooth and TiO_2 particles are agglomerated in SMPU as shown in Fig. 2 (d). This is because TiO_2 nanoparticles have large specific surface area, and there are many active sites on the surface which leads to the surface energy in an unstable state. It is easy to agglomerate and reach a stable balanced state which may affect other test results of crystallization behaviors, shape memory effects, mechanical properties, etc [21].

3.3 Crystallization behaviors

To investigate the influence of TiO_2 contents on crystallization behaviors and phase structurs of

TiO_2/SMPU nanocomposites, WAXD tests are conducted on the TiO_2, SMPU and TiO_2/SMPU samples, respectively. The test results are illustrated in Fig. 3.

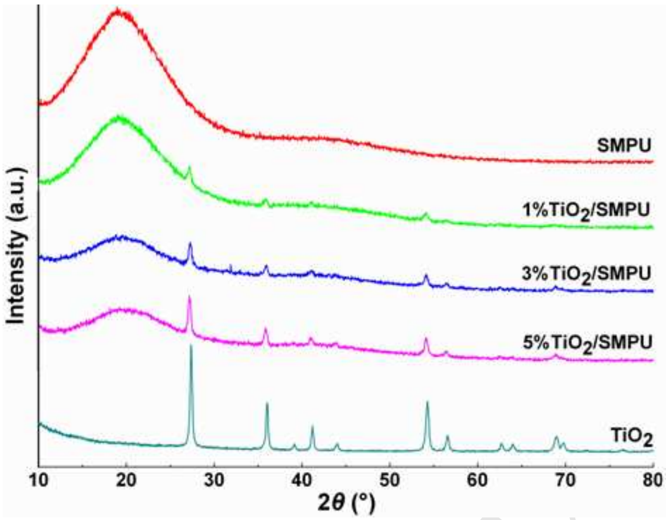

Fig. 3 WAXD patterns of TiO_2, SMPU and TiO_2/SMPU composites with different TiO_2 contents

As shown in Fig. 3, pure SMPU shows a broad diffused diffraction peak at around 2θ=19°, indicating that SMPU is typical of amorphous polymeric materials, and there are amorphous phases or microcrystals in SMPU. This may be due to the fact that the crystals formed by the polymer are usually microcrystalline structures, and their crystallite sizes are small [22]. Another reason is attributed to the the aggregation of chain segments because of microphase separation in SMPU [23]. Also, when the different contents of TiO_2 are added into SMPU, five main characteristic diffraction peaks of TiO_2 are still seen at 27.4°, 36.0°, 41.2°, 54.3° and 69.0°, respectively. Compared with TiO_2 standard card (JCPDS No: 21-1276), it is found that TiO_2 used in this study is rutile phase.

From Fig. 3, it is noted that the intensity of characteristic diffraction peak of TiO_2/SMPU at 2θ=19° is decreased gradually and the peak become weaker and broader with the increase in TiO_2 content. This is because TiO_2 nanoparticles affect the motion of molecular chains in SMPU and then the orderness of chain segments is decreased and it is difficult to form a stable aggregation state [24]. Therefore, this leads to the decrease in crystallinity of TiO_2/SMPU, and the intensities of diffraction peaks become weaker.

Furthermore, the diffraction peaks also appear at 27.4°, 36.0°, 41.2°, 54.3° and 69.0° in the WAXD patterns of TiO_2/SMPU nanocomposites, and the intensities of diffraction peaks are increased gradually with the increase in TiO_2 content. It suggests that the characteristic diffraction peaks of TiO_2 exist in TiO_2/SMPU nanocomposites. This indicates that TiO_2 nanoparticles are successfully filled in SMPU matrix and they still retain the original crystal structures in the compositses [25].

3.4 Optical properties

In order to study effects of TiO_2 nanoparticles on optical properties of SMPU, the UV–Vis DRS tests are carried out on pure SMPU and TiO_2/SMPU nanocomposites. UV-Vis absorption spectra of TiO_2/SMPU nanocomposites with different TiO_2 contents are shown in Fig. 4.

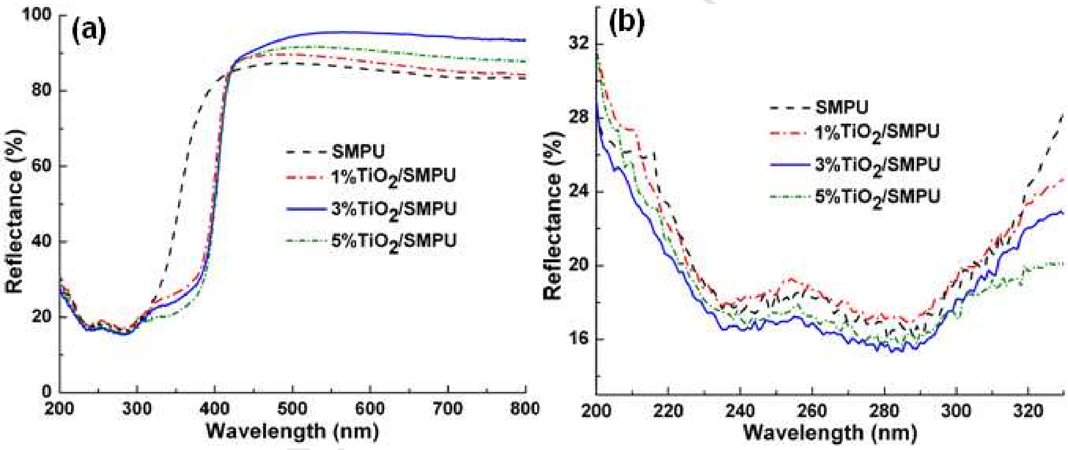

Fig. 4 (a) UV-Vis reflection spectra of TiO_2/SMPU nanocomposites with different TiO_2 contents and (b) enlarged subplot in UV light region

As shown in Fig. 4 (a), pure SMPU has a larger reflectance in the UV light region than TiO_2/SMPU nanocomposites. After the TiO_2 nanoparticles are incorporated in SMPU matrix, the reflectance of TiO_2/SMPU nanocomposites is decreased in the UV light region, particularly in the wavelength range from 310 nm to 400 nm. This is because that the rutile TiO_2 used in this study belongs to the n-type semiconductor with a wide band gap, which is composed of low energy band (valence band) with full of electrons and high energy band (conduction band) without electrons [5]. Under the stimulation of UV light, the electrons of valence band absorb energy to jump to conduction band. This makes TiO_2 to absorb more UV light so that the UV reflectance of TiO_2/SMPU nanocomposites is decreased. This effectively lowers the degradation and photo-aging of SMPU due to the absorption of UV light.

Fig. 4 (b) further presents that the UV reflectance of 1%TiO_2/SMPU sample is similar to that of pure SMPU, and the UV reflectance of 3%TiO_2/SMPU sample is smaller than those of 1%TiO_2/SMPU and 5%TiO_2/SMPU samples. This is because the TiO_2 content of 1% is too small to have obvious effects on the reflectance of TiO_2/SMPU nanocomposites. Another reason is some TiO_2 nanoparticles in 5%TiO_2/SMPU sample is agglomerated as shown in Fig. 2 (d), which affects the UV reflectance of TiO_2/SMPU. Additionally, from Fig. 4 (a), it is noted that the UV-Vis reflection spectra of TiO_2/SMPU nanocomposites present a red shift. This may be due to the fact that the UV light absorption range of TiO_2 is wider, thus expanding the absorption range of TiO_2/SMPU nanocomposites [26].

In the visible light region, pure SMPU reflectance to visible light is about 85%, while the reflectance of TiO_2/SMPU nanocomposites is increased. Particularly, the reflectance of 3%TiO_2/SMPU sample reaches the maximum value of 95%. The possible reason is that the reflectivity of TiO_2 crystal face is stronger. The reflectivity of 5%TiO_2/SMPU sample is lower, which is attributed to the partial agglomeration of TiO_2 nanoparticles.

It is concluded that the suitable TiO_2 content can improve the UV light absorptance and visible light reflectance of TiO_2/SMPU nanocomposites. When the TiO_2 content is 3%, the absorptivity to UV light and the reflectivity to visible light of TiO_2/SMPU reach the maximum values. The absorbed UV light is transformed into heat to emit from TiO_2/SMPU nanocomposites, which can lower the damages to the SMPU molecular chains due to UV light absorption. The reflectivity of TiO_2 to visible light can also lowered the photo-aging properties of TiO_2/SMPU nanocomposites, thus prolonging its service life.

3.5 Microstructural and interfacial characterization

The SAXS technique is used to obtain microstructural and interfacial information of pure SMPU and representative 3%TiO_2/SMPU. 2D-SAXS patterns of the above two samples are shown in Fig. 5.

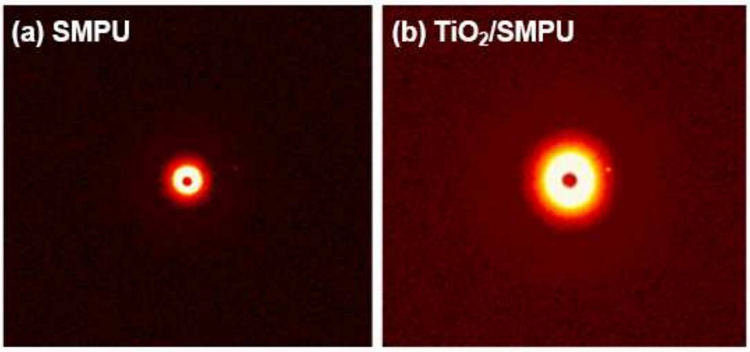

Fig. 5 2D-SAXS patterns of pure SMPU and representative TiO_2/SMPU nanocomposites

As shown in Fig. 5 (a), 2D-SAXS patterns of SMPU show isotropic scattering haloes since the scattering densities of hard and soft segments are different. It indicates the presence of periodic isotropic structures due to the microphase separation in SMPU [27]. This is because hard and soft segments are randomly curled in the SMPU. From Fig. 5 (b), 2D-SAXS patterns of TiO_2/SMPU are quite similar to that of SMPU, but the scattering intensity of TiO_2/SMPU is obviously increased. The reason for this is that the composite material is isotropic and the spherical scatters of TiO_2 nanoparticles exist [28].

The corresponding SAXS profiles such as scattering curves and azimuthal intensities of pure SMPU and representative 3%TiO_2/SMPU nanocomposites are illustrated in Fig. 6.

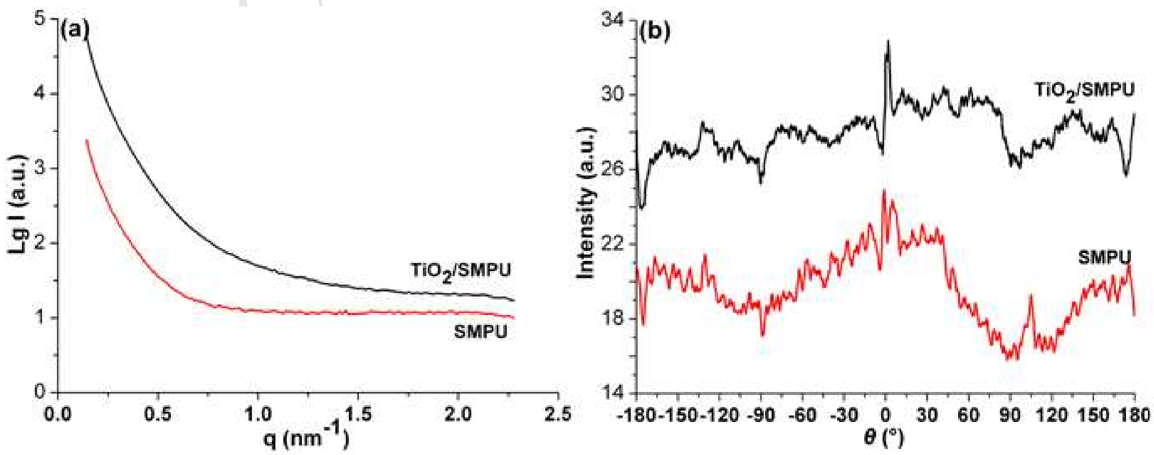

Fig.6 SAXS profiles of (a) scattering curves and (b) azimuthal intensities of pure SMPU and

representative 3%TiO_2/SMPU nanocomposites

It is seen from Fig.6 that the scatting intensity of TiO_2/SMPU is higher than that of SMPU. This is because that the number of scatters is increased after the addition of TiO_2 in SMPU, and the X-ray is scattered by spherical TiO_2 nanoparticles with crystal structures, leading to the increase in scattering intensity of TiO_2/SMPU [29]. This indicates that the increase in scattering intensity is mainly attributed to the addition of TiO_2 nanoparticles.

Additionally, the scatting intensity of SMPU shows a decreasing trend with the increase in scattering vector (q), suggesting there is an electron density difference between soft and hard segments in SMPU. This is because of the microphase separation between soft and hard segments which is derived from their mutual repulsion and respective aggregation in SMPU. Similarly, the scatting intensity of TiO_2/SMPU shows a more obvious decreasing trend with the increase in scattering vector (q). It indicates that there is a larger electron density difference between TiO_2 nanoparticles and SMPU matrix. This is attributted to the larger difference in material properties between inorganic TiO_2 and organic SMPU matrix.

As shown in Fig. 6 (b), SMPU and TiO_2/SMPU samples show similar scattering peaks. However, the scattering peaks of SMPU are stronger than those of TiO_2/SMPU, particularly, and there is a broader and stronger scattering peak at around θ=0^o. This suggests that the microphase separation of soft and hard segments in SMPU is affected by addition of TiO_2 nanoparticles, and the ordered structures in SMPU are decreased, forming more disordered structures in SMPU. The reasons for this are the interface interaction between TiO_2 and SMPU and steric-hinerance effects affect the aggregation of hard phase in SMPU [30].

Furthermore, more intermediate phase is formed between TiO_2 nanoparticles and SMPU matrix, leading to the decrease in miscrophase separation of SMPU. This is because TiO_2 nanoparticles have a huge specific surface area and high surface energy although its content is small. SMPU molecular chains are adsorbed on the TiO_2 nanoparticle surface to lower their surface energy. TiO_2

nanoparticles are coated and anchored by organic molecular chains of SMPU. The mutual diffusion, permeation and entanglement occur between SMPU molecular chains and TiO_2 nanoparticles, generating the intermediate phase interface structures [30].

To further understand the interfacial structures in the above two samples, the microstructure characteristics are investigated by classical SAXS theory according to SAXS scattering curves [28]. It is known that Porod approximation is suitable to discuss the interface information of different phases [31]. Porod curves from SAXS test results of SMPU and representative 3%TiO_2/SMPU are given in Fig. 7.

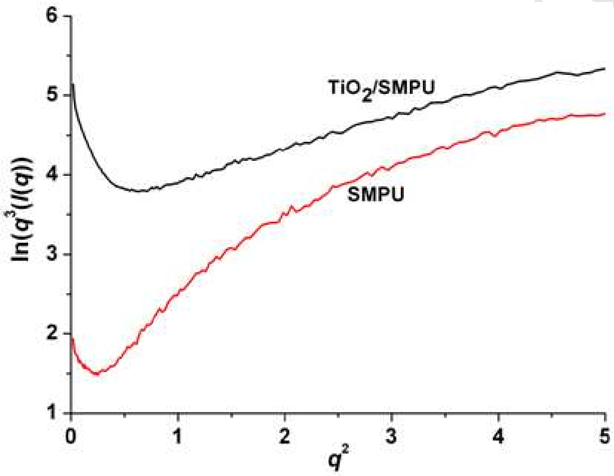

Fig. 7 Porod curves of pure SMPU and representative 3%TiO_2/SMPU nanocomposites

Fig. 7 shows the typical plot of $\ln[q^3I(q)]$ versus q^2 from SAXS test results of SMPU and representative 3%TiO_2/SMPU samples. It is seen that the plot of 3%TiO_2/SMPU sample is different from that of SMPU, indicating the addition of TiO_2 leads to the changes in electronic energy states. It is noted that the SAXS intensity plots of both SMPU and TiO_2/SMPU nanocomposites do not conform to the Porod theorem [28], and show the typical positive deviations at the high angles. Further, the positive deviations of the above two samples gradually tend to similarity. This indicates that there are electron density fluctuations at the interfaces between hard and soft phases in SMPU, and between SMPU matrix and TiO_2 nanoparticles in TiO_2/SMPU nanocomposites. The electron density fluctuations show no obvious difference at the high angles.

For TiO_2/SMPU nanocomposites, it is believed that the interface interaction between organic SMPU molecular chains and inorganic TiO_2 nanoparticles is responsible to the positive deviation. On the one hand, there may be Debye shielding layer causes positive and negative charges on TiO_2 nanoparticle surface to redistribute [32]. The distribution of positive and negative charges is not a gradual gentle transition process from the inside of nanoparticles to SMPU matrix, but it is a shielding process with jumping characteristics. This results in the local electron density fluctuation at the interface between TiO_2 and SMPU matrix because the electrons at the interface are interfered by opposite charges [32].

Also, a large number of traps are formed at the interface due to the incorporation of inorganic TiO_2 nanoparticles, which leads to the generation of space charges, affecting the electron density in the interface between TiO_2 nanoparticles and SMPU [32]. Similarly, for pure SMPU, the distribution of positive and negative charges is not a gentle transition process at the interface between the hard and soft phases of SMPU. The electrons at the interface are interfered by opposite charges to cause the local electron density fluctuation. Also, the formed traps at the interface lead to electron density changes.

3.6 Shape memory effects

To study effects of TiO_2 contents on the shape memory effects of SMPU, the shape memory properties of TiO_2/SMPU with different TiO_2 contents are characterized by R_f and R_r. The test results of R_f and R_r of TiO_2/SMPU samples with different TiO_2 contents are within the standard deviations, and the average values of R_f and R_r are presented in Table 1.

Table 1 Test results of shape memory effects of TiO_2/SMPU specimens with different TiO_2 contents

TiO_2 content (%)	l_0 (mm)	l_1 (mm)	l_2 (mm)	l_3 (mm)	R_f	R_r
0.0	40.0	42.7	42.7	40.0	100%	100%
1.0	40.0	43.0	43.0	40.0	100%	100%
3.0	40.0	43.2	43.1	40.1	96.9%	96.8%
5.0	40.0	42.9	42.7	40.2	93.1%	92.6%

From Table 1, it is found that both R_f and R_r of pure SMPU and 1%TiO_2/SMPU specimens are 100%, indicating that a small amount of TiO_2 nanoparticles has few effects on the shape memory properties of SMPU. Both R_f and R_r of 3%TiO_2/SMPU and 5%TiO_2/SMPU specimens are slightly less than those of pure SMPU and 1%TiO_2/SMPU specimens. This suggests that the shape memory properties of SMPU are lowered as the TiO_2 content is further increased. The resons for this are that the addition of TiO_2 nanoparticles loweres the crystallization of soft segments in SMPU, and thus affects the R_f of SMPU. At the same time, the added TiO_2 nanoparticles in the composite system prevent the hard phase from recovering to its original states, and this resistance is increased with the increase in TiO_2 content. Therefore, both R_f and R_r of TiO_2/SMPU nanocomposites are decreased. However, it is noted that both R_f and R_r of TiO_2/SMPU nanocomposites are larger than 90%, indicting that the prepared TiO_2/SMPU nanocomposites have better shape memory effects.

3.7 Mechanical properties

Effects of TiO_2 content on tensile properties of SMPU are discussed here since it is obvious that the compressive performance of SMPU is improved after reinfored by TiO_2 nanoparticles. Test results of tensile stress-strain responses of TiO_2/SMPU with different TiO_2 contents are given in Fig. 8.

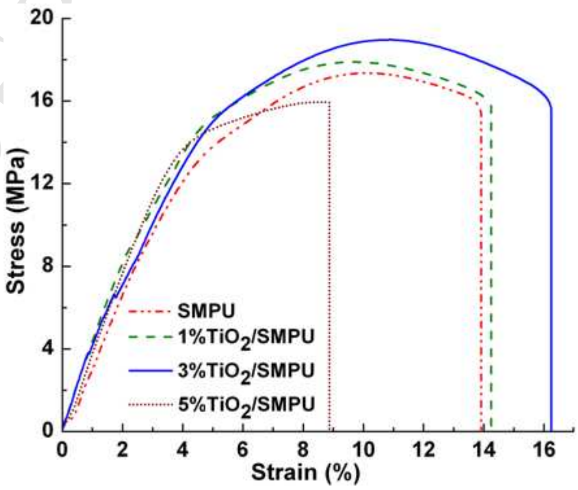

Fig. 8 Tensile stress-strain responses of TiO_2/SMPU composites with different TiO_2 contents

As shown in Fig. 8, both tensile strength and elongation at break of TiO_2/SMPU nanocomposites are first increased and then decreased as the TiO_2 content is increased from 0% to 5%. The 3%TiO_2/SMPU specimen shows the highest tensile properties. This is mainly because SMPU belongs to the foam materials, and there are a lot of tiny pores in SMPU matrix. When a small amount of TiO_2 is added in SMPU, these nanoparticles are filled in the tiny pores. The obvious size and surface effects of TiO_2 nanoparticles lead to a close combination with SMPU matrix, thus the intermolecular interaction force is improved. Thus when the TiO_2/SMPU specimen is in tension, the tensile strength and elongation at break of the nanocomposites are increased.

However, TiO_2 nanoparticles are not uniformly dispersed in SMPU matrix as TiO_2 content is more than 3%. The formed agglomeration of TiO_2 nanoparticles affect the motion and orderness of molecular chains so local defects are easily generated in TiO_2/SMPU nanocomposites. This leads to the stress concentration in TiO_2/SMPU nanocomposites during the tension test, and then the tensile strength and elongation at break are lowered.

4. Conclusions

In this study, TiO_2/SMPU nanocomposites with different rutile TiO_2 contents are prepared, and their various properties are characterized and discussed. The main conclusions are obtained as follows.

(1) The melting temperature of soft segments in SMPU is used as the shape memory T_t of TiO_2/SMPU. It is lowered as TiO_2 content is increased, but showing a slight influence on the T_t. All shape memory T_ts of TiO_2/SMPU are at around 55^{o}C, and the programming temperature is proposed at 65 ^{o}C.

(2) The prepared SMPU is porous structures. All pores are almost filled up when TiO_2 content is 3%, and TiO_2 nanoparticles are wrapped by SMPU to form compact skeleton structures in TiO_2/SMPU. Some agglomerations are found as TiO_2 content is up to 5% which affect test results of crystallization behaviors, optical performance, shape memory effects, mechanical properties, etc.

(3) The added rutile TiO_2 lowers the crystallinity of SMPU and decreases the diffraction peak intensity of TiO_2/SMPU. TiO_2 retains its original crystal structures in TiO_2/SMPU. The suitable TiO_2 content can improve the absorptivity to UV light and increase the reflectivity to visible light of TiO_2/SMPU. This improves the anti-aging properties of TiO_2/SMPU, thus prolonging its service life.

(4) Both SMPU and TiO_2/SMPU show similar isotropic 2D-SAXS scattering patterns, but the scattering intensity of TiO_2/SMPU is obviously higher than that of pure SMPU. SAXS profile of TiO_2/SMPU present a more obvious decreasing trend than that of SMPU due to the larger electron density difference between TiO_2 nanoparticles and SMPU matrix.

(5) The microphase separation in SMPU is affected by the addition of TiO_2 nanoparticles, and ordered structures in SMPU are decreased. SAXS intensity plots of SMPU and TiO_2/SMPU do not conform to Porod law, showing typical positive deviations. There are electron density fluctuations at the interfaces between hard and soft phases, and between SMPU and TiO_2 in TiO_2/SMPU.

(6) Both R_f and R_r of TiO_2/SMPU are decreased with the increase in TiO_2 content, but they are larger than 90% even if TiO_2 content reaches 5%. Prepared TiO_2/SMPU nanocomposites have better shape memory effects. The tensile properties of TiO_2/SMPU are improved by adding a suitable TiO_2 content. TiO_2 content of 3% is proposed to prepare TiO_2/SMPU nanocomposites.

Acknowledgements

Authors would like to thank the financial support from National Natural Science Foundation of China (No.51378264), and the Doctorate Fellowship Foundation of Nanjing Forestry University (2169040), and Provincial Six Talent Peaks Project in Jiangsu (Grant No. JNHB-050), and the Priority Academic Program Development of Jiangsu Higher Education Institutions (PAPD). Also we would like to thank Advanced Analysis & Testing Center of Nanjing Forestry University for the assistance in experiments.

References

[1] Z.D. Lu, A.F. Wu, X.M. Ou, Enhanced anti-aging and mechanical properties of polyamide 1010 by sol-hydrothermal titanium dioxide-coated kaolinite addition, J. Alloys Compd. 693 (2017) 381–388.

[2] S.D. Mo, W.Y. Ching, Electronic and optical properties of three phases of titanium dioxide: Rutile, anatase, and brookite, Phys. Rev. B. 51 (19) (1995) 13023–13032.

[3] H. Mehranpour, M. Askari, M.S. Ghamsari, Study on the phase transformation kinetics of sol-gel drived TiO_2 nanoparticles, J. Nanomater. 2010 (6) (2010) 31–36.

[4] B. Ingham, S. Dickie, H. Nanjo, In situ USAXS measurements of titania colloidal paint films during the drying process, J. Colloid Interface Sci. 336 (2) (2009) 612–615.

[5] C. Man, C. Zhang, Y Liu, Poly(lactic acid)/titanium dioxide composites: Preparation and performance under ultraviolet irradiation, Polym. Degrad. Stab. 97 (6) (2012) 856–862.

[6] T. Gong, W. Li, S. Zhou, Remotely actuated shape memory effect of electrospun composite nanofibers, Acta Biomater. 8 (2012) 1248–1259.

[7] G.Q. Li, A. Wang, Cold, warm, and hot programming of shape memory polymers, J. Polym. Sci., Part B: Polym. Phys. 54 (14) (2016) 1319–1339.

[8] Y. Liu, Y. Li, S. Zhou, Multi-stimulus-responsive shape-memory polymer nanocomposite network cross-linked by cellulose nanocrystals, ACS Appl. Mater. Interfaces 7 (2015) 4118−4126.

[9] J. Hu, C. Zhang, F. Ji, X. Li, Revealing the morphological architecture of a shape memory polyurethane by simulation, Scientific Reports , 6(2016)29180–29190.

[10] L. Hou, Y. Ding, Z. Zhang, Synergistic effect of anionic and nonionic monomers on the synthesis of high solid content waterborne polyurethane, Colloids Surf. A 467 (2015) 46–56.

[11] W. Wang, D. Liu, S. Zhou. The improvement of the shape memory function of poly (3-caprolactone)

/cellulose nanocomposites via recrystallization, J. Mater. Chem. A 4 (2016) 5984–5992.

[12] H. Zhou, Y. Chen, H. Fan, Water vapor permeability of the polyurethane/TiO_2 nanohybrid membrane with temperature sensitivity, J. Appl. Polym. Sci. 109 (2008) 3002–3007.

[13] Y. Chen, R. Wang, J Zhou, Membrane formation temperature-dependent gas transport through thermo- sensitive polyurethane containing in situ-generated TiO_2, Polymer 52 (2011) 1856– 1867.

[14] P. Zhang, T. Kraus, Anisotropic nanoparticles as templates for the crystalline structure of an injection-molded isotactic polypropylene/TiO_2 nanocomposite, Polymer 130 (2017) 161–169.

[15] M.A. Marzouk, F.H. ElBatal, H.A. ElBatal, Effect of TiO_2 on the optical, structural and crystallization behavior of barium borate glasses, Opt. Mater. 57 (2016) 14–22.

[16] M.L.P. Ramos, J.A. González, G.J. Copello, Chitin hydrogel reinforced with TiO2 nanoparticles as an arsenic sorbent, Chem. Eng. J. 285 (2016) 581–587.

[17] S. Shi, D. Shen, T. Xu, Microstructural and mechanical property evolutions of shape memory polyurethane during a thermodynamic cycle, J. Appl. Polym. Sci. 135(2017) 45703–45713.

[18] S.J. Hong, H.Y. Ji, W.R. Yu, Determination of the transition temperature of shape memory polyurethanes using constrained recovery test, Fibers Polym. 11 (5) (2010) 749–756.

[19] S.R. Armstrong, J. Du, E. Baer, Co-extruded multilayer shape memory materials: Nano-scale phenomena. Polymer 55(2) (2014) 626–631.

[20] J.T. Garrett, R. Xu, J. Cho, Phase separation of diamine chain-extended poly (urethane) copolymers, FTIR spectroscopy and phase transitions, Polymer 44 (9) (2003) 2711–2719.

[21] L. Xu, Y. Fu, M. Du, Investigation on structures and properties of shape memory polyurethane/Silica Nanocomposites, Chin. J. Chem. 29 (4) (2011) 703–710.

[22] J. Xu, W. Shi, W. Pang, Synthesis and shape memory effects of Si–O–Si cross-linked hybrid

polyurethanes, Polymer 47 (1) (2006) 457–465.

[23] J.W. Cho, H.L. Sun, Influence of silica on shape memory effect and mechanical properties of polyurethane–silica hybrids, Eur. Polym. J. 40 (7) (2004) 1343– 1348.

[24] Y.H. Yun, K.J. Hwang, Y.J. Wee, Synthesis, physical properties, and characterization of starch-based blend films by adding nano-sized TiO_2, J. Appl. Polym. Sci. 120 (3) (2011) 1850–1858.

[25] M. Sadeghi, H.T. Afarani, Z. Tarashi, Preparation and investigation of the gas separation properties of polyurethane-TiO_2 nanocomposite membranes, Korean J. Chem. Eng. 32 (1) (2015) 97–103.

[26] N. Erdem, U.H. Erdogan, A.A. Cireli, Structural and ultravioletprotective properties of nano-TiO_2-doped polypropylene filaments, J. Appl. Polym. Sci. 115 (1) (2010) 152–157.

[27] H. Koerner, J.J. Kelley, R.A. Vaia, Transient microstructure of low hard segment thermoplastic polyurethane under uniaxial deformation, Macromolecules 41 (13) (2008) 4709–4716.

[28] X.X. Liu, J.H. Yin, Y.N. Kong, The property and microstructure study of polyimide/nano-TiO_2 hybrid films with sandwich structures, Thin Solid Films 554 (10) 2013 54–58.

[29] C. Bartholome, E. Beyou, E. Bourgeat-lami, Viscoelastic properties and morphological characterization of silica/polystyrene nanocomposites synthesized by nitroxide-mediated polymerization, Polymer, 46 (23) (2005) 9965–9973.

[30] S. Asiaban, S.F. Taghinejad. Investigation of the effect of titanium dioxide on optical aspects and physical characteristics of ABS polymer, J. Elastomers Plast. 42 (42) (2010) 267–274.

[31] A. Turković, Grazing-incidence SAXS/WAXD on nanosized TiO_2 films obtained by ALE, Mater. Sci. Eng. B 75 (1) (2000) 85–91.

[32] Y. Feng, J.H. Yin, M.H. Chen, Effect of nano-TiO_2 on the polarization process of polyimide/TiO_2 composites, Mater. Lett. 96 (4) (2013) 113–116.